Anderson William Jr, RE Emanuel (2008) Effect of interannual and interdecadal climate oscillations on groundwater in North Carolina, Geophys Res Lett 35:L23402, doi:10.1029/2008GL036054. Version of record available from Wiley [ISSN: 1944-8007], [DOI: 10.1029/2008GL036054]

Effect of interannual and interdecadal climate oscillations on groundwater in North Carolina

[1] Multi-year climate oscillations such as the El Niño–Southern Oscillation (ENSO) and Pacific Decadal Oscillation (PDO) affect precipitation and stream discharge rates in the western hemisphere. While inferences may be drawn between these hydroclimatological relationships and groundwater conditions, few studies explicitly link groundwater conditions to these cycles. Here we investigate relationships between winter ENSO, PDO, and lagging baseflow rates in the southeastern United States. We find strong correlation between winter ENSO and lagged baseflow in coastal North Carolina which, coupled with anomalies in mean baseflow, decrease with distance inland from the coast. Our results demonstrate that interannual and interdecadal climate oscillations in the Pacific Ocean have a strong effect on hydrological processes in eastern North America despite filtering by the groundwater flow process. These results have implications for water resource availability in regions where water management is complicated by population growth and climatic uncertainty.
Citation: Anderson, W. P., Jr., and R. E. Emanuel (2008), Effect of interannual and interdecadal climate oscillations on groundwater in North Carolina, *Geophys. Res. Lett.*, *35*, L23402, doi:10.1029/2008GL036054.

1. Introduction

[2] The past decade has seen a preponderance of research on the link between interannual and interdecadal climate oscillations such as ENSO and PDO, respectively, and a wide variety of hydrological processes. These studies range from an examination of the correlation between these signals and the magnitude and timing of snowmelt runoff in Oregon [*Beebee and Manga*, 2004] and assessment of the correlation between rainfall erosivity and ENSO [*D'Odorico et al.*, 2001] to direct examination of interannual climate oscillation-precipitation relationships [*Rajagopalan and Lall*, 1998; *Kwon et al.*, 2006], interdecadal climate oscillation-precipitation relationships [*Lucero and Rodríquez*, 1999], and interdecadal climate oscillation-streamflow relationships [*Gutiérrez and Dracup*, 2001]. Little research, however, investigates the relationship between climate oscillations and groundwater resources hypothesized by *Rodell and Famiglietti* [2001]. Studies addressing this relationship mainly focus on the western United States, Canada, and the Pacific [*Fleming and Quilty*, 2006; *Hanson et al.*, 2004; *Drexler and Ewel*, 2001; *van der Velde et al.*, 2006]. No study documenting the relationship between groundwater conditions and climatic signals has been undertaken in the southeastern United States, although previous research indicates that a relationship exists between climate signals and precipitation in this region. For example, *Roswintiarti et al.* [1998] identify precipitation anomalies in eastern North Carolina during January and July of the 1998 El Niño event. *Kurtzman and Scanlon* [2007] define a region of characteristically wet El Niño winters through the southern tier of the United States that extends marginally into North Carolina.

[3] Enhanced recharge during winter months, when evapotranspiration is at a minimum, may be a significant source of groundwater storage [*Anderson and Evans*, 2007]; groundwater conditions during subsequent months and seasons may depend on the previous winter's precipitation. *Rodell and Famiglietti* [2001] demonstrate the connection between winter recharge and groundwater storage, noting that groundwater storage lags soil moisture by zero to two months with average conditions falling during summer months and rising during winter months. *Eltahir and Yeh* [1999] show similar lag times. Analysis of groundwater conditions on Hatteras Island, North Carolina, as a precursor to this study, suggests the importance of winter recharge. Winter (DJF) recharge fractions derived from calibrated groundwater flow and transport simulations average 62%; summer (JJA) recharge fractions average 31%. Mean seasonal values of groundwater levels and baseflow rates calculated for this study also show this seasonality.

[4] Given the importance of winter precipitation to groundwater storage, correlations between measured groundwater parameters and interannual and interdecadal climate oscillations may enable predictions of groundwater availability under forecasted climate conditions. Furthermore, reanalysis of six years of daily water-level data collected over a period of twelve years on Hatteras Island suggests at least some causal link between ENSO and groundwater levels. Significant correlation (Spearman's $\rho = 0.724$, $p = 0.001$) between the Multivariate ENSO Index (MEI) [*Wolter and Timlin*, 1998] and mean seasonal groundwater levels, as well as relative groundwater-level anomalies of greater than 50% prompt us to expand upon previous work and explore in greater detail potential teleconnections between ENSO, PDO, precipitation, and groundwater conditions.

2. Methods

[5] We use data from December 1949 to the present from weather stations (accessed from http://www.ncdc.noaa.gov/oa/climate/stationlocator.html between November 7, 2007 and January 8, 2008) and stream gauges (accessed from http://water.usgs.gov/waterwatch/ on the same range of dates) throughout central and eastern North Carolina and

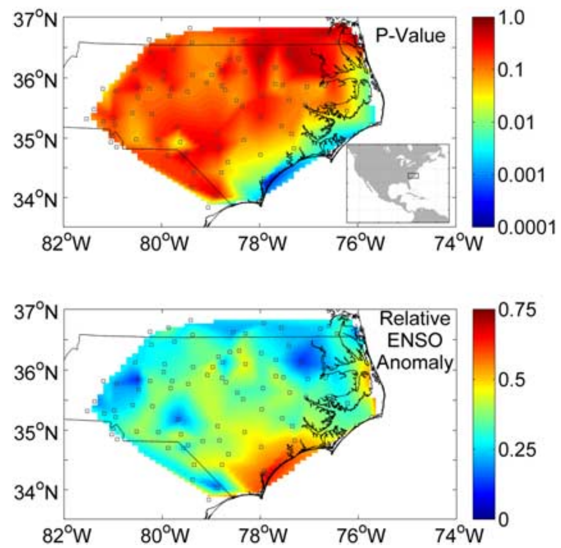

Figure 1. Influence of winter ENSO on winter precipitation interpolated across 94 meteorological stations (boxes). (top) Significance of Spearman's rank correlation between winter (DJF) MEI and winter precipitation generally decreases with distance from Atlantic coast as shown by a contour plot of p values. (bottom) ENSO-induced precipitation anomaly generally decreases with distance from the coast.

adjacent states. December 1949 corresponds with the initial date of the bi-monthly average MEI (accessed from http://www.cdc.noaa.gov/people/klaus.wolter/MEI/table.html during November 2007). Precipitation and stream gauges lacking more than 12 months of data were eliminated from analyses. To maintain consistency with the MEI signal we convert monthly precipitation totals, monthly average stream data, and calculated monthly average baseflow data to bi-monthly averages. We convert all of these data, along with the MEI signal, to seasonal averages (*e.g.*, DJF for winter). We convert seasonal hydrologic datasets to standard deviation units and calculate their correlations to seasonal MEI using Spearman's rank correlation (ρ). We calculate seasonal anomalies in hydrologic parameters between extremes in El Niño and La Niña signals using differences between upper and lower quartiles of MEI following *Kurtzman and Scanlon* [2007]. We also examine the effect of PDO alone and its combined effect with ENSO on sampled parameters. We compute the El Niño Decadal Modulation (ENDM) and the La Niña Decadal Modulation (LNDM) by splitting datasets into roughly equal-length PDO phases to: a cold phase from 1950 to 1977, and a warm phase from 1978 to 2007 [*Hanson et al.*, 2004]. The ENDM (LNDM) reflects the relative influence of PDO on the El Niño (La Niña) positive (negative) baseflow anomaly [*Kurtzman and Scanlon*, 2007]. We calculate the ENDM (LNDM) modulations for each of our sites and during all seasons using the upper (lower) quartile of MEI values during both phases of PDO. We determine the most significant lag in MEI-baseflow correlation by computing a weighted average of ENSO-induced baseflow anomalies by watershed area.

[6] We calculate monthly baseflow rates from stream discharge at gauging stations across the study region using the sliding-interval hydrograph separation technique [*Risser et al.*, 2005; *Sloto and Crouse*, 1996]. We use baseflow as a proxy for groundwater because long, continuous time-series of water-level data are unavailable in our study region. We also use baseflow because unlike water-level data, which represent groundwater conditions at a single point, baseflow represents groundwater conditions averaged over an entire watershed. Where monthly water-level data exist, they correlate well with variations in baseflow (ρ = 0.84, p < 0.01). Calculated baseflow ratios for 29 of our sites have a mean of 0.611 and range from 0.419 to 0.829. These values are consistent with baseflow ratios computed in previous studies [e.g., *Eltahir and Yeh*, 1999].

3. Results and Discussion

[7] Our analysis of 56 years of precipitation data from 94 stations demonstrates a significant positive correlation between winter MEI and winter precipitation that is strongest at stations located near the Atlantic coast and decays inland (Figure 1 (top)). ENSO conditions significantly influence winter precipitation at all seven stations within 50 km of the coast and 12 of the 17 stations within 100 km of the coast (Figure 1 (top)). We observe up to 67% more winter precipitation during strong El Niño conditions (upper quartile MEI) than during strong La Niña conditions (lower quartile MEI). These winter precipitation anomalies are greatest at stations located near the coast and decrease inland, averaging 34% across the study area and reaching a minimum of 11% at a distance of 315 km from the Atlantic coast (Figure 1 (bottom)). These results along with previous studies [*Roplewski and Halpert*, 1987; *Gershunov*, 1998] demonstrate the influence of ENSO on winter precipitation. This influence forms the connection between ENSO and groundwater in this region, which in turn explains correlations between MEI and baseflow. The correlation between precipitation and baseflow for the 17 of 30 total study basins that contain one or more rain gauges are significant (p < 0.01) at all locations, during all seasons, and at all lags. Mean ρ values from zero to three months lag range from 0.52 to 0.80, with a maximum single-site correlation of 0.91.

[8] During the winter months (0 lag), ENSO exerts a significant influence (p < 0.05) on baseflow at nine of the 30 stations, but when a time lag for infiltration of the climate signal is considered, this number rises to 13, 18, and 21 stations at one-, two-, and three-months lag, respectively. When computing a weighted-average based on watershed area, a two-month lag in baseflow represents the peak of the winter ENSO influence across the study area (Figure 2). Moreover, for each set of lag correlations (0 to 3 months), we find an increase in correlation moving from northwest to southeast across the study area. This pattern mimics the pattern in the correlation between ENSO and precipitation across the same region. This trend and the peaking correlation at two months' lag in baseflow suggest not only that precipitation is the mechanism by which the ENSO signal is transmitted to groundwater, but also that the earth's surface and subsurface play a role in modulating the magnitude and timing of this signal.

[9] The ENSO-related baseflow anomaly at two months' lag reflects the difference between mean values during

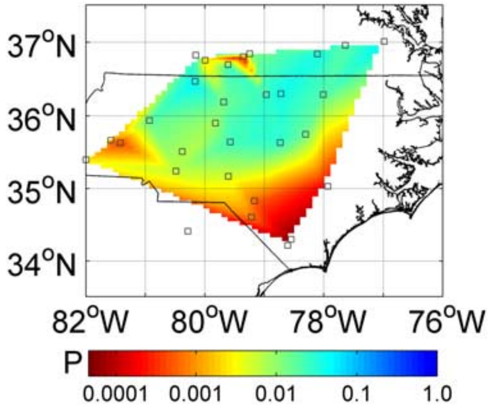

Figure 2. Influence of winter (DJF) ENSO on baseflow in 30 watersheds across the region. *P*-values of Spearman's rank correlation between MEI and baseflow are interpolated from centroids of watersheds (boxes) for 2-month lag (FMA) in baseflow.

upper and lower quartiles relative to mean winter baseflow (Figure 3a). These anomalies approach 100% in the southeastern portion of the study area but decrease with distance from the southeast coast, a condition similar to that of the precipitation trend (see Figure 1 (bottom)). Baseflow anomalies between the PDO warm and cold phases are also a function of mean winter baseflow. The PDO anomaly is much smaller in magnitude than the ENSO anomaly, fluctuating about zero throughout the study area (Figure 3b).

[10] The negative and positive trends in the PDO anomaly affect the region's ENDM. The southern coastal region shows negative ENDM, suggesting that the PDO warm phase reduces the positive ENSO anomaly during El Niño conditions (Figure 3c). The large positive ENDM anomaly in the northern coastal region suggests that the PDO warm

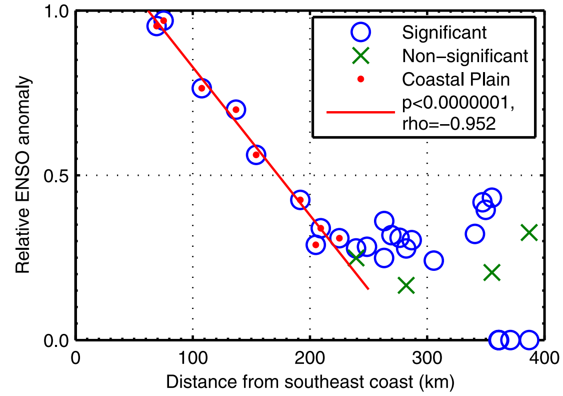

Figure 4. Influence of winter (DJF) ENSO on one-month lagged baseflow anomalies versus distance from the southeast coast of North Carolina. The figure denotes significant (circles) and non-significant (crosses) stations. For significant Coastal Plain stations (open circles) we show linear regression.

phase modulates the ENSO anomaly in this region. These results differ from the findings of *Kurtzman and Scanlon* [2007], who identified only negative ENDM throughout North Carolina. While our LNDM results also differ from those of *Kurtzman and Scanlon* [2007], who found only low positive to negative LNDM in eastern North Carolina, they are similar in suggesting that at two-months lag, PDO modulates the baseflow response to ENSO more with La Niña than with El Niño (Figure 3d). This modulation by way of LNDM applies only to the Coastal Plain of North Carolina (east of the broken line in Figure 3). All of western North Carolina experiences negative LNDM. The dominant combined effect of PDO and ENSO on the region is to further reduce baseflow in the Coastal Plain during La Niña conditions.

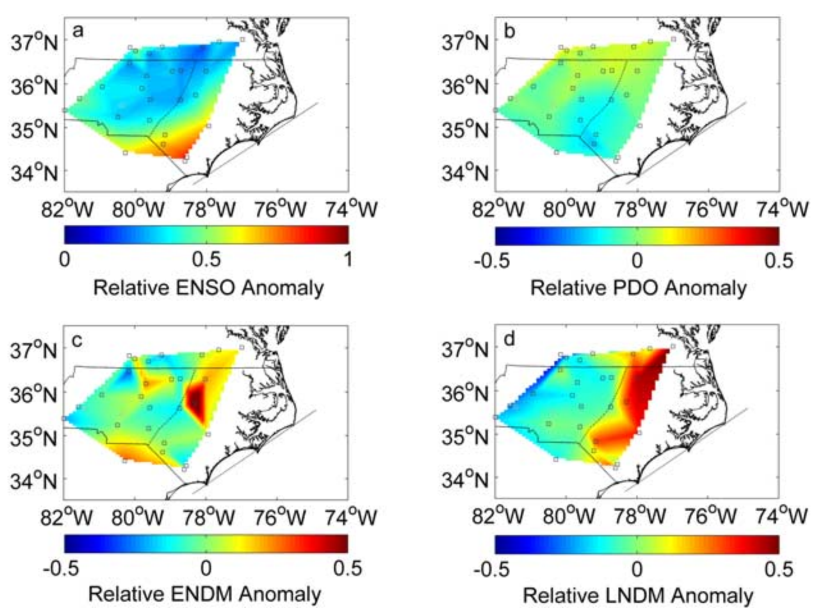

Figure 3. Influence of winter (DJF) ENSO, PDO, and combined effect of ENSO and PDO on winter baseflow anomalies with 2-month lag in 30 watersheds across the region. Relative anomalies are interpolated from centroids of watersheds (dark boxes) for (a) ENSO, (b) PDO, (c) ENDM, and (d) LNDM. The approximate boundary between the Piedmont and Coastal Plain (dot-dash line) and the orientation of the strongest correlation (dashed line) are shown in each plot.

[11] Noting the strong inland-trending decline in the relative ENSO anomaly, we compare these same anomalies as a function of distance from the southeast coast at one-month lag, which has the highest individual correlations between baseflow and ENSO. The strong decay through the Coastal Plain of North Carolina is evident in a plot of the relative ENSO anomaly as a function of distance from the southeast coast (Figure 4). Extrapolation to the coast suggests an anomaly greater than 100%, which decays sharply to 25% at the Coastal Plain - Piedmont boundary. The decrease in relative ENSO anomaly with distance inland is highly significant for the Coastal Plain ($p < 10^{-7}$, $\rho = -0.952$). Baseflow trends inland at two- and three-month lags are also significant, but not as extreme. Baseflow anomalies in the Piedmont are approximately 25% at all lags.

[12] A sharp change in the trend of the relative ENSO anomaly occurs at the transition from the Coastal Plain to the Piedmont (Figure 4). While we have demonstrated that precipitation is a driving factor in the teleconnection of the ENSO signal to the groundwater reservoir, contrasting hydrogeology in the study area may also be a contributing factor. Coastal Plain surficial aquifers comprise layered sedimentary materials that are, in general, highly-permeable and easily-recharged during the winter. The ease of infiltration of the precipitation-derived, ENSO-correlated recharge anomaly may be responsible for the large baseflow anomalies at relatively short time lags in the Coastal Plain. In contrast, Piedmont aquifers comprise low-permeability fractured bedrock aquifers that are overlain by thick, clayey soils. Therefore, the water-table response of Piedmont aquifers to recharge events may not be as dynamic because of decay in the precipitation teleconnection combined with the diffusive effects of low permeability aquifers. In summary, the strength of the connection between the climate oscillation and baseflow is believed to be primarily driven by climate (precipitation). Further study is required before a more definitive correlation can be made with respect to the strength of the hydrogeologic filtering.

[13] This work suggests that that groundwater resource availability in the southeast United States may be predicted based on interannual climate oscillations. This is the first demonstration of the relationship between the ENSO signal and groundwater conditions in this region. Recent droughts and increasing groundwater demands from growing coastal populations, mining, irrigation, and livestock operations are straining finite water resources. The consequences of rising groundwater usage are aquifer dewatering, saltwater intrusion, and land subsidence [*North Carolina Rural Economic Development Center*, 2002]. Large groundwater pumping rates during periods of ENSO-related low-flow conditions may exacerbate these problems; therefore, the ability to use climate signals to forecast groundwater resource availability may help to alleviate some of these demands through conservation and planning. Consequently, the results of our analyses have implications for the management of groundwater supplies in regions affected by ENSO variability in addition to improving our understanding of teleconnections between global-scale climate signals and regional hydrological processes.

References

Anderson, W. P., Jr., and D. G. Evans (2007), On the interpretation of recharge estimates from steady-state model calibrations, *Ground Water*, *45*(4), 499–505, doi:10.1111/j.1745-6584.2007.00312.x.

Beebee, R. A., and M. Manga (2004), Variation in the relationship between snowmelt runoff in Oregon and ENSO and PDO, *J. Am. Water Resour. Assoc.*, *40*(4), 1011–1024.

D'Odorico, P., J.-C. Yoo, and T. M. Over (2001), An assessment of ENSO-induced patterns of rainfall erosivity in the southwestern United States, *J. Clim.*, *14*, 4230–4242.

Drexler, J. Z., and K. C. Ewel (2001), Effect of the 1997–1998 ENSO-related drought on hydrology and salinity in a Micronesian wetland complex, *Estuaries*, *24*(3), 347–356.

Eltahir, E. A. B., and P. J.-F. Yeh (1999), On the asymmetric response of aquifer water level to floods and droughts in Illinois, *Water Resour. Res.*, *35*(4), 1199–1217.

Fleming, S. W., and E. J. Quilty (2006), Aquifer responses to El Niño–Southern Oscillation, southwest British Columbia, *Ground Water*, *44*(4), 595–599.

Gershunov, A. (1998), ENSO influence in intraseasonal extreme rainfall and temperature frequencies in the contiguous United States: Implications for long-range predictability, *J. Clim.*, *11*, 3192–3203.

Gutiérrez, F., and J. A. Dracup (2001), An analysis of the feasibility of long-range streamflow forecasting for Colombia using El Niño–Southern Oscillation indicators, *J. Hydrol.*, *246*, 181–196.

Hanson, R. T., M. W. Newhouse, and M. D. Dettinger (2004), A methodology to assess relations between climatic variability and variations in hydrologic time series in the southwestern United States, *J. Hydrol.*, *287*, 252–269.

Kurtzman, D., and B. R. Scanlon (2007), El Niño–Southern Oscillation and Pacific Decadal Oscillation impacts on precipitation in the southern and central United States: Evaluation of spatial distribution and predictions, *Water Resour. Res.*, *43*, W10427, doi:10.1029/2007WR005863.

Kwon, H.-H., U. Lall, Y.-I. Moon, A. F. Khalil, and H. Ahn (2006), Episodic interannual climate oscillations and their influence on seasonal rainfall in the Everglades National Park, *Water Resour. Res.*, *42*, W11404, doi:10.1029/2006WR005017.

Lucero, O. A., and N. C. Rodríquez (1999), Relationship between interdecadal fluctuations in annual rainfall amount and annual rainfall trend in a southern mid-latitudes region of Argentina, *Atmos. Res.*, *52*, 177–193.

North Carolina Rural Economic Development Center (2002), Water woes in eastern North Carolina: Facing the facts, reaching solutions, N. C. Rural Econ. Dev. Cent., Raleigh, N. C.

Rajagopalan, B., and U. Lall (1998), Interannual variability in western US precipitation, *J. Hydrol.*, *210*, 51–67.

Risser, D. W., W. J. Gburek, and G. J. Folmar (2005), Comparison of methods for estimating ground-water recharge and base flow at a small watershed underlain by fractured bedrock in the eastern United States, *U.S. Geol. Surv. Sci. Invest. Rep.*, 2005–5038.

Rodell, M., and J. S. Famiglietti (2001), An analysis of terrestrial water storage variations in Illinois with implications for the Gravity Recovery and Climate Experiment (GRACE), *Water Resour. Res.*, *37*(5), 1327–1339.

Roplewski, C. F., and M. S. Halpert (1987), Global and regional scale precipitation patterns associated with the El Niño–Southern Oscillation, *Mon. Weather Rev.*, *115*, 1606–1626.

Roswintiarti, O., D. S. Niyogi, and S. Raman (1998), Teleconnections between tropical Pacific sea surface temperature anomalies and North Carolina precipitation anomalies during El Niño events, *Geophys. Res. Lett.*, *25*(22), 4201–4204.

Sloto, R. A., and M. Y. Crouse (1996), HYSEP: A computer program for streamflow hydrograph separation and analysis, *U.S. Geol. Surv. Water Resour. Invest. Rep.*, *96-4040*.

van der Velde, M., M. Javaux, M. Vanclooster, and B. E. Clothier (2006), El Niño–Southern Oscillation determines the salinity of the freshwater lens under a coral atoll in the Pacific Ocean, *Geophys. Res. Lett.*, *33*, L21403, doi:10.1029/2006GL027748.

Wolter, K., and M. S. Timlin (1998), Measuring the strength of ENSO—How does 1997/98 rank?, *Weather*, *53*, 315–324.